FORMATION OF CERES' MASCONS. A.I. Ermakov[1] (eai@berkeley.edu), B.C. Johnson[2], R. S. Park[3]; J. C. Castillo-Rogez[3]; [1]Space Sciences Laboratory, University of California, Berkeley, 94720; [2]Purdue University, West Lafayette, IN, 47907; [3]Jet Propulsion Laboratory, California Institute of Technology, Pasadena, CA, 91011.

Introduction: The dwarf planet Ceres is the largest object in the asteroid belt. The Dawn mission has found that Ceres' surface is heavily cratered. The two biggest unambiguous impact craters are Kerwan with a radius of 284 km [1] and Yalode with a radius of 260 km [2]. The Dawn gravity and shape data allow investigating the subsurface structure of these features. The latest gravity model of Ceres is globally accurate up to spherical harmonic degree n=18 (spatial wavelength of 164 km) [3]. However, the effective resolution of the gravity model reaches n=59 within the Urvara crater-third largest crater with a diameter of 160 km.

Crustal inversions (**Fig. 1**) using gravity and shape data show a superisostatic mantle uplift (i.e., crust-mantle interface perturbation in excess of the prediction from an isostatic model) in the center of Kerwan [4]. A similar structure is observed in Yalode. However, the Yalode anomaly pattern is less symmetric with respect to the crater center. Correspondingly, the crust at the center of the craters is estimated to be thinner than for the case of pure isostatic compensation and the exterior annulus presents an overthickened crust.

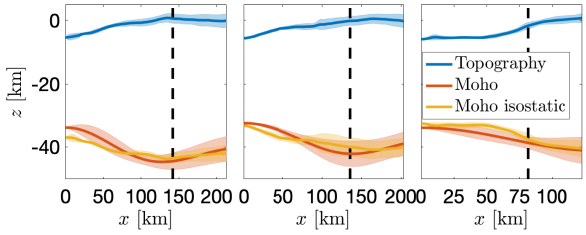

Figure 1: Averaged radial profiles for the topography and crust-mantle boundary computed from the crustal thickness inversion [4] for Kerwan, Yalode and Urvara craters (left to right). The isostatic crust-mantle boundary is also shown. The shaded region indicates 1σ error bars.

Urvara, on the other hand, is not a mascon. The isostatic anomaly at Urvara is negative and the Bouguer anomaly is positive. Therefore, Urvara is partially compensated, implying that the crustal thinning beneath Urvara is not strong enough to create a mascon. Thus, we observed the transition from supercompensated craters or mascons (Kerwan and Yalode) to partially compensated craters (Urvara) and uncompensated craters such as Dantu and Zadeni. This observation is similar to the lunar basins that develop a bullseye mascon pattern in isostatic anomaly only when a certain diameter is reached [5].

The goals of this study are: 1) to test if the lunar-like mascon formation mechanism can explain cerean mascons; 2) to constrain the rheological and thermal parameters of cerean crust and upper mantle that are required to support the observed superisostatic state of impact craters.

Impact Modeling: We use *iSALE-2D* to model the formation of cerean large craters. The *iSALE-2D* shock physics code [6] is based on the *SALE* hydrocode solution algorithm [7]. To simulate hypervelocity impact processes in solid materials, *SALE* was modified to include an elastic-plastic constitutive model, fragmentation models, various equations of state, and various materials [8,9].

To reduce computational expense, we utilize axisymmetric models. We consider a vertical impact at a typical impact velocity of 4.8 km/s [10]. The target has a surface temperature of 150 K and surface gravity of 0.27 m/s^2. The lithospheric thermal gradient was varied within the range 0.5-3 K/km to find suitable matches to crater crustal thickness profiles.

For the crust, we use the material strength parameters and mixed material appropriate for cerean ice/rock (water ice and serpentine) mixture that were used by [11]. Crustal thickness inversions [4] based on Dawn's gravity measurement suggest Ceres has an approximately 40-km thick crust with a density of 1300 kg/m^3 overlying a denser mantle (2400 kg/m^3). We expect that the gravity signatures of large craters are sensitive to the mantle, which is represented by serpentine in our simulations.

Viscoelastic Relaxation Modeling: The final state of the impact modeling serves as an input to the finite-element modeling of crater's relaxation and cooling. Our modeling setup is based on the previous studies of topography relaxation of Vesta [12] and Ceres [13].

The horizontal extent of the mesh is 400 km, which is chosen such that the boundary condition does not significantly alter the flow inside the crater. The vertical extent of the mesh is 150 km. We use the Lagrangian approach, in which the movement of the mesh follows the movement of the material. We apply the free surface boundary condition at the top, free slip on the left, bottom and right boundary.

We use simple Newtonian rheology in form of an Arrhenius relationship:

$$\eta(T) = \eta_0 \exp\left(\frac{E_a}{RT_0}\left(\frac{T_0}{T} - 1\right)\right), \quad (1)$$

where η_0 is the reference viscosity, T_0 is the reference temperature, R is the universal gas constant and T is the material temperature. Since the rheological properties of the cerean crust and mantle are highly uncertain, we take

the parameter of Eq. 1 appropriate for water ice and vary η_0 to mimic a rock-like rheology.

The thermal evolution is solved simultaneously with the Stokes flow. The material properties such as heat capacity and thermal conductivity are taken from ice-rock mixture data [14]. The heat conduction is solved using the Crank-Nicolson scheme. The time step is chosen to satisfy two conditions. The maximum mesh displacement in one time step is set to a fraction of the cell size. The time step is also limited by the Courant–Friedrichs–Lewy (CFL) condition for the heat conduction.

Modeling Results: We have explored the parameter space of mascon formation in several directions to identify the key control parameters. We have varied conductivity, heat capacity, thermal expansion coefficient and reference viscosity of the crust and mantle. We have also varied the thermal expansion coefficient of the crust and the mantle.

The factors that control crater's cooling and relaxation are: 1) gravity, which determines the buoyancy force that drives the viscous flow; 2) viscosity, which determines the material resistance to flow; and 3) diffusivity, which determines how quickly the impact heat dissipates. Time of impact could be another factor controlling the formation and evolution of an impact crater, as younger Ceres likely had a steeper thermal gradient. The temporal evolution of viscosity is mostly set by the thermal conductivity. If thermal conductivity is high, the impact heat is dissipated quickly, effectively limiting the isostatic adjustment of the crater. The key parameter that controls the rate of isostatic adjustment is the reference viscosity, which in our simple model, acts as a scale factor for viscosity.

We find Ceres' mascons do not form with the same mechanism as was proposed for the Moon [15,16]. On the Moon, a large amount of impact melt and post-impact sloshing lead to a compensated initial state of large basins [17]. Impact melting is more limited for Cerean craters and the target maintains sufficient strength to support a post-impact superisostatic anomaly. A lower gravity on Ceres also means that it is easier to support a non-isostatic structure. For Kerwan and Yalode, we find that the mantle uplift can freeze in a super-isostatic state following the collapse of the transient cavity (**Fig. 2**). This is similar to the original mascon formation idea for the Moon [18], before it was realized that lunar basins would be immediately isostatically compensated. Thus, our task is to find the parameters that can preserve this superisostatic state over geologic time scales. We find that a reference viscosity of $\eta_0 > 10^{19}$ Pa s is needed to preserve superisostatic crater centers over 100's of My, which corresponds to about 3 orders of magnitude larger surface viscosity compared to the topographic relaxation study of [13]. This could potentially be explained by rock and salt inclusions into Ceres' crust effectively inhibiting relaxation, which is consistent with experimental data of [19], who conducted deformation experiments of the ice-rock mixture and concluded that only a small fraction of rock particles is required to inhibit grain boundary sliding reducing effective viscosity. In addition, we plan to incorporate the effect of plasticity in our modeling similarly to [13], which would likely reduce the effective viscosity through plastic failure.

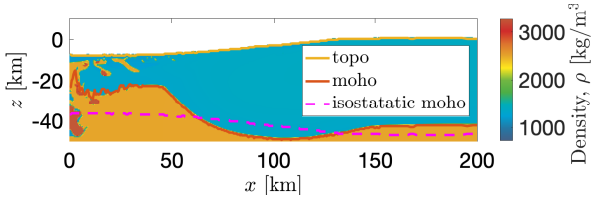

Figure 2: Post-impact state of Kerwan-like crater. "Moho" refers to the crust-mantle boundary, whereas "isostatic moho" refers to the crust-mantle boundary assuming isostatic compensation. A super-isostatic mantle uplift is evident since the crust-mantle boundary is above the isostatic moho at the center of the crater.

Acknowledgments: This work was carried out in part at the Jet Propulsion Laboratory, California Institute of Technology, under contract with the National Aeronautics and Space Administration. This research was funded through NASA's Discovery Data Analysis Program.

References: [1] Williams D. et al. (2018) *Icarus*, 316, 99–113; [2] Crown D. et al., (2018) *Icarus*, 316, 167–190; [3] Park, R.S. et al. (2020) *Nature Astronomy*, 4(8), 748–755; [4] Ermakov A.I. et al., (2017) *JGR:Planets*, 122(11), 2267–2293; [5] Andrews-Hanna, Andrews-Hanna, J.C. (2013) *Icarus*, 222(1), 159-168; [6] Wünnemann K. et al. (2006) *Icarus*, 180(2), 514–527; [7] Amsden A. (1980) (Tech. Rep.). Los Alamos Scientific Lab., NM (USA); [8] Melosh H. et al. (1992) *JGR:Planets*, 97(E9), 14735–14759; [9] Ivanov B. et al. (1997) *International Journal of Impact Engineering*, 20(1-5), 411–430; [10] Hiesinger H. et al. (2016) *Science*, 353(6303), aaf4759; [11] Bowling T. et al. (2019) *Icarus*, 320, 110–118; [12] Fu R. et al. (2014) *Icarus*, 240, 133–145; [13] Fu R. et al. (2017) *EPSL*, 476, 153–164; [14] Barnhart C. et al. (2010) *Icarus*, 208(1), 101–117; [15] Melosh H. et al. (2013) *Science*, 340(6140), 1552–1555; [16] Freed A. et al. (2014) *JGR:Planets*, 119(11), 2378–2397; [17] Pierazzo E. and Melosh H. (2000) *An Rev of Earth and Planetary Sci,* 28(1), 141–167; [18] Neumann G. et al. (2004) *JGR:Planets*, 109(E8); [19] Qi C. et al. (2018) *GRL*, 45(23), 12–757;